Kinetic Folding and *Cis*/*Trans* Prolyl Isomerization of Staphylococcal Nuclease. A Study by Stopped-Flow Absorption, Stopped-Flow Circular Dichroism, and Molecular Dynamics Simulations†

Teikichi Ikura, Galina P. Tsurupa, and Kunihiro Kuwajima*

Department of Physics, School of Science, University of Tokyo, Hongo, Bunkyo-ku, Tokyo 113, Japan

Received December 27, 1996; Revised Manuscript Received March 28, 1997⊗

ABSTRACT: We studied the urea-induced unfolding transition of staphylococcal nuclease (SNase) and its five proline mutants (P47A, P47T, P117G, P47A/P117G, and P47T/P117G) by peptide and aromatic circular dichroism and aromatic absorption spectroscopy at equilibrium and the refolding−unfolding kinetics of the proteins by stopped-flow circular dichroism and stopped-flow absorption techniques. Recent studies have revealed that the *cis*/*trans* isomerizations about the Pro47 and Pro117 peptide bonds of SNase occur not only in the unfolded state but also in the native state. The mutational effects on the stability and the refolding−unfolding kinetics of SNase were, however, remarkably different between the two sites. The substitution of Ala or Thr for Pro47 neither changed the stability nor affected the refolding−unfolding kinetics of SNase, whereas the substitution of Gly for Pro117 increased the protein stability by 1.2 kcal/mol (pH 7.0 and 20 °C) and affected the kinetics. These results have been attributed to the high flexibility of the loop around Pro47, which has been revealed by molecular dynamics simulations of native SNase. Under every condition studied, cooperative refolding−unfolding kinetics of SNase were observed. Refolding of wild-type SNase was represented by two urea concentration-dependent fast phases and a urea concentration-independent slow phase. The double mutant (P47A/P117G) of SNase still showed multiphasic refolding kinetics that involved two urea concentration-independent slow phases, suggesting that isomerization of proline residues other than Pro47 and Pro117 may occur in the unfolded state of the mutant. Two phases were observed in the unfolding of the wild-type and mutant proteins that contained Pro117, a fast phase corresponding to the unfolding of the *trans* isomer and a slow phase corresponding to that of the *cis* isomer. On the basis of these results, the folding scheme of SNase is discussed.

Elucidating the molecular mechanism of protein folding from the unfolded (U) state to the native (N) state remains one of the major challenges in biochemistry. Although the information required for folding a protein to the N state is apparently encoded in the protein's amino acid sequence (Anfinsen, 1973), it is difficult to resolve the protein folding problem, due to the complexity of the free energy landscape of the conformational space available for a protein, i.e., the availability of an astronomically large number of different conformations and the presence of a large number of local minima on the energy surface (Bryngelson et al., 1995; Dill et al., 1995; Levinthal, 1968; Onuchic et al., 1995; Scheraga, 1996). Nevertheless, studies of protein folding kinetics have succeeded in characterizing the rate-limiting steps of the folding reactions in many globular proteins and have revealed the presence of partially folded intermediates at an early stage of refolding from the U state (Baldwin, 1993; Kim & Baldwin, 1990; Kuwajima, 1989, 1996), intermediates which may or may not be obligatory, on-pathway intermediates of folding (Baldwin, 1996). The refolding of most globular proteins has been characterized by multiphasic kinetics, which have been ascribed to the presence of partially folded intermediates or multiple parallel folding pathways (Miranker & Dobson, 1996). For many proteins, however, they are also explained by isomerization of X−Pro peptide bonds in the U state (Brandts et al., 1975; Kiefhaber et al., 1992; Kiefhaber & Schmid, 1992; Kim & Baldwin, 1982). Although such isomerization may play a significant role in *in vitro* and *in vivo* protein folding, it does not directly reflect the real folding events. Thus, the solution of the protein folding problem requires that such isomerization, if it occurs, should be identified and discriminated from real folding events.

Among proteins studied for the isomerization of X−Pro peptide bonds, staphylococcal nuclease (SNase)[1] is one of the best characterized. This protein is known to exhibit proline isomerization in not only the U but also the N state, and this gives rise to structural heterogeneity in the N state. According to the NMR studies of SNase, this structural heterogeneity can be ascribed to the isomerizations about the Lys116−Pro117 (Alexandrescu et al., 1989, 1990; Evans et al., 1989; Fox et al., 1986; Hinck et al., 1993) and His46−Pro47 peptide bonds (Loh et al., 1991). In native wild-type SNase, the predominant configuration (about 90%) of the Lys116−Pro117 peptide bond is assigned to *cis* and the

† This work was supported by Grants-in-Aid for Scientific Research from the Ministry of Education, Science and Culture of Japan and by a Research Grant from the International Human Frontier Science Program (HFSP) Organization (RG-331/93M). G.P.T. is a JSPS (Japan Society for the Promotion of Science) Postdoctoral Fellow.

* To whom correspondence should be addressed.

⊗ Abstract published in *Advance ACS Abstracts,* May 15, 1997.

[1] Abbreviations: SNase, staphylococcal nuclease; EDTA, ethylenediamine-*N*,*N*,*N*′,*N*′-tetraacetic acid; EGTA, [ethylenebis(oxyethylenenitrilo)]tetraacetic acid; GdnHCl, guanidine hydrochloride; CD, circular dichroism; rmsd, root mean square displacement; GdnSCN, guanidine thiocyanate; C^{α}, α-carbon; pdTp, thymidine 3′,5′-disphosphate.

S0006-2960(96)03174-1 CCC: $14.00

minor configuration (about 10%) is assigned to *trans* (Alexandrescu et al., 1989, 1990; Evans et al., 1989). For the His46−Pro47 peptide bond, the major configuration (about 80%) is assigned to *trans* whereas the minor configuration (about 20%) is assigned to *cis* (Loh et al., 1991). In the previous study, we have shown, as a preliminary result, that the biphasic unfolding kinetics of wild-type SNase changed into single-phasic kinetics by the substitution of Gly for Pro117 (Kuwajima et al., 1991; Sugawara et al., 1991), indicating that the heterogeneity in the N state was eliminated by the substitution.

In the present study, in addition to this single mutant of Pro117 (P117G), we prepared two single mutants of Pro47, in which Pro47 was replaced by Ala and Thr (P47A and P47T), and two double mutants of Pro47 and Pro117 (P47A/P117G and P47T/P117G). We studied the urea-induced equilibrium unfolding transition and the refolding−unfolding kinetics of wild-type and mutant SNase. The results show that the effects of the mutations on the stability and the refolding−unfolding kinetics of the protein are remarkably different between the two mutation sites. The substitution of Ala or Thr for Pro47 did not change the protein stability nor the refolding−unfolding kinetics of the protein, whereas the substitution of Gly for Pro117 increased the protein stability and affected both the refolding and unfolding kinetics of the protein. Molecular dynamics simulations for wild-type SNase were carried out both *in vacuo* and in water. The simulations revealed a remarkable difference between the flexibilities of structures around Pro47 and Pro117, and we used this difference to explain the similar disparity in the mutational effects between the two sites. It was also found that, under every condition studied, the rate constants and relative amplitudes for the refolding and unfolding kinetics of the protein measured by the stopped-flow absorption and the stopped-flow circular dichroism (CD) techniques were identical, indicating cooperative refolding and unfolding of SNase. Refolding kinetics of wild-type SNase were represented by two urea concentration-dependent fast phases and a urea concentration-independent slow phase. The double-mutant SNase (P47A/P117G) still showed multiphasic refolding kinetics that involved two urea concentration-independent slow phases. Thus, isomerization of other proline residues or other isomerization events may occur in the U state. From these results, the folding scheme of SNase is discussed.

MATERIALS AND METHODS

Chemicals. Urea was of a specially prepared reagent grade for biochemical use from Nacalai Tesque, Inc. (Kyoto). Urea stock solution was deionized on a mixed-bed column of Amberlite IR-120B and IRA-402 and used within several days. The concentration of urea was determined from the refractive index at 589 nm (Pace, 1986) with an Atago 3T refractometer. All other chemicals were of guaranteed reagent grade.

Proline Mutants of Staphylococcal Nuclease. The gene of wild-type SNase from the Foggi strain of *Staphylococcus aureus* and the gene of its mutant P117G were obtained from recombinant plasmids (pDRS113-SNase and pDRS113-SNase-P117G; Kuwajima et al., 1991) by the PCR method (Saiki et al., 1988). Expression plasmids (pMT7-SN and pMT7-SN-P117G) were constructed by inserting the gene fragments of wild-type SNase and the mutant P117G between the *Nco*I and *Sal*I sites of an expression vector (pMT7) containing T7 promoter and M13 intergenic regions; pMT7 is a hybrid of pUC118 and a plasmid pUT7 that was a gift from I. Kumagai. Expression plasmids containing mutations P47A, P47T, P47A/P117G, and P47T/P117G were constructed from single-stranded pMT7-SN and pMT7-SN-P117G and mutagenic primers by using either of the two mutagenesis kits, an "Oligonucleotide-directed *in vitro* mutagenesis system version 2" (Amersham Inc.) (Sayers et al., 1988) and a "MUTA-GENE phagemid *in vitro* mutagenesis kit" (BIO-RAD) (Kunkel, 1985). The nucleotide sequences of the mutant plasmids were identified by an ALF express autosequencer (Pharmacia).

Protein Purification. To prepare wild-type SNase and its mutants, their expression plasmids were transformed into competent BL21(DE3)/pLysS cells (Novagen, Inc.). Two milliliters of overnight preculture of the *Escherichia coli* cells, supplemented with both chloramphenicol (34 μg/mL) and ampicillin (50 μg/mL), was inoculated into 1 L of 2× YT medium supplemented with the same antibiotics in a 5 L flask, and this culture was grown to the log phase (OD at 600 nm was 0.4−0.5). Overproduction of the protein was initiated by addition of isopropyl β-D-thiogalactopyranoside to 1 mM. The culture was grown for an additional 4 h, and the cells were collected by centrifugation. The cell pellet was once frozen at −20 °C and then thawed slowly at room temperature. The cell pellet was suspended in 50 mM Tris-HCl buffer (pH 8.0) that contained 1 mM EDTA, 100 mM sodium chloride, and 133 μM phenylmethanesulfonyl fluoride (3 mL of the buffer per 1 g of the pellet). The cells were then lysed by sonication for 10 min at 200 W with an Insonator 201M sonicator (Kubota, Inc.). The cell debris was removed by centrifugation, and ammonium sulfate was added to the cleared lysate to 35% saturation. After the precipitate was removed by centrifugation, further ammonium sulfate was added into the supernatant to 80% saturation. The precipitate was collected by centrifugation and dissolved in an appropriate volume of 100 mM ammonium acetate buffer (pH 8.0) that contained 6 M guanidine hydrochloride (GdnHCl) and 10 mM dithiothreitol. The mixture was incubated for 1 h at room temperature. The precipitate was removed by centrifugation, and the supernatant was filtered through a Millipore membrane filter (type HV) with a pore size of 0.45 μm and then passed through a Sephacryl S-100 column equilibrated with 100 mM ammonium acetate buffer (pH 8.0). The column was washed with 1 column volume of the same buffer, and the eluant was fractionated by a fraction collector. The fractions containing SNase were collected. The collected solution was lyophilized and dissolved in an appropriate volume of 50 mM Tris-HCl buffer (pH 8.0). The solution was loaded onto an S Sepharose FF column, which had been equilibrated with the same buffer. The column was then washed with 1 column volume of the same buffer followed by 4 column volumes of the additional buffer with a linear gradient of NaCl from 0 to 0.5 M. The fractions containing SNase were collected, concentrated by ultrafiltration, and again passed through a Sephacryl S-100 column equilibrated with 100 mM ammonium acetate buffer (pH 8.0), and the purified protein solution was lyophilized.

Sample Preparation. The lyophilized protein was first dissolved in 50 mM sodium cacodylate buffer (pH 7.0) that

contained 50 mM NaCl, 1 mM [ethylenebis(oxyethylenenitrilo)]tetraacetic acid (EGTA), and a high concentration of urea (typically 8 M). Urea was included for the purpose of completely dissociating aggregated SNase; SNase has a marked tendency to aggregate [see Kalnin and Kuwajima (1995)]. The solution (2 mL) was filtered through a Millipore membrane filter (MILLEX-HV) with a pore size of 0.45 μm and was applied on an 8 mL Sephadex G-25 column (NAP-25, Pharmacia) equilibrated with 50 mM sodium cacodylate (pH 7.0) plus 50 mM NaCl, 1 mM EGTA, and an appropriate amount of urea, if required. The concentrations of wild-type and mutant SNase were determined by UV absorption using an extinction coefficient $E^{1\%}_{1cm}$ of 9.3 at 280 nm (Tucker et al., 1978).

Equilibrium Measurements. Equilibrium CD spectra were taken on a Jasco J-720 spectropolarimeter using an optical cuvette with a path length of 1.00 mm for measurements in the peptide region and 10.0 mm for measurements in the aromatic region. The mean residue ellipticity was calculated by taking 113 as the mean residue weight (Tucker et al., 1978). Equilibrium difference absorption spectra were taken on a Jasco UVIDEC-430B spectrophotometer using an optical cuvette with a path length of 10.0 mm. All measurements were carried out at 20 °C. The concentration of the protein for the equilibrium measurements was 0.3−0.5 mg/mL.

Kinetic Measurements. Refolding and unfolding reactions of wild-type and mutant SNase were induced by urea concentration jumps, which were performed by two stopped-flow apparatus (UNISOKU Co., Japan): a stopped-flow CD apparatus installed in the cell compartment of the J-720 spectropolarimeter and a stopped-flow absorption apparatus (Arai & Kuwajima, 1996; Kuwajima et al., 1996). All kinetics were measured at 20 °C. The dead times of the measurements were 26 ms for the stopped-flow absorption apparatus and 23 ms for the stopped-flow CD apparatus. The concentration of the protein stock solution was about 1 mg/mL. The initial protein solution before the concentration jump contained 1.0 and 4.5 M urea for the unfolding and refolding experiments, respectively. The diluent solution contained the same buffer and salts and an appropriate concentration of urea. The two solutions were mixed with a mixing ratio of 1:9 (stopped-flow absorption) or 1:10 (stopped-flow CD) (protein:diluent).

Molecular Dynamics Simulations. Molecular dynamics simulations of SNase were carried out with a DISCOVER 95.0 module of an INSIGHT II package (Biosym Technologies, Inc., San Diego) on an IRIS indigo^2 (Silicon Graphics, Inc.). The CFF91 force field for the protein molecule and the TIP3P model for water were employed (Jorgensen et al., 1983). The X-ray crystal structure 1STN was adopted as the initial conformation because its coordinates were determined at a high resolution (1.70 Å) and because it was crystallized without Ca^{2+} and pdTp (Hynes & Fox, 1991). Polar hydrogen atoms were added to the coordinates of the X-ray crystal structure of SNase with a BUILDER module of the INSIGHT II package. The structure was minimized by 400 steps of the conjugate gradient algorithm of energy minimization; the rmsd from the X-ray structure was 0.4 Å for the backbone heavy atoms and 0.5 Å for all heavy atoms. Standard molecular dynamics simulation was carried out *in vacuo* and also in a rectangular box (46.7 × 46.7 × 62.0 Å^3) consisting of 4041 water molecules under a periodic boundary condition. The temperature of the system was controlled by the velocity scaling method. For the dielectric constant, the value *in vacuo* was used. The nonbonding cutoff distance was 10 Å for both the van der Waals interactions and the electrostatic interactions. In the simulation *in vacuo*, the system was first equilibrated at 293 K for 100 ps, and the subsequent 100 ps trajectory was studied. In the simulation in water, the system equilibration was first carried out at 293 K for 50 ps and then at 327 K [the experimental denaturation temperature at neutral pH (Tanaka et al., 1993)] for 50 ps, and the subsequent 100 ps trajectory was studied at 327 K. For both cases, a time step of 1 fs was employed with the Verlet leapfrog integration algorithm (Verlet, 1967), and the structure was stored in the computer every 1 ps.

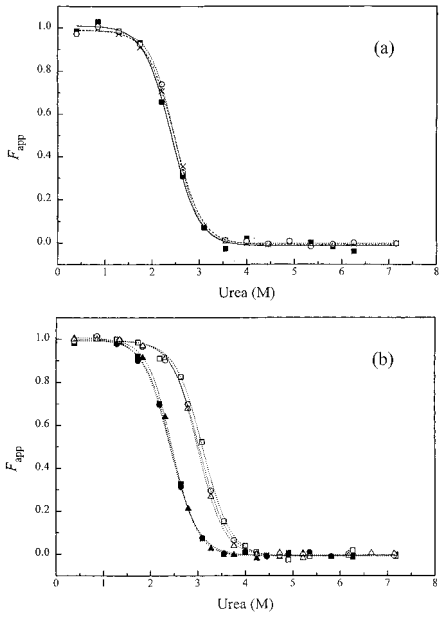

FIGURE 1: Equilibrium unfolding transition of wild-type SNase and its proline mutants at pH 7.0 and 20 °C. (a) The apparent fraction of native species (F_{app}) for wild-type SNase at each urea concentration is plotted. Symbols and lines represent the F_{app} values and the unfolding transition curves, respectively, measured by the difference absorption at 292.5 nm (■ and solid line), the CD at 225 nm (× and dashed line), and the CD at 276 nm (○ and dotted line). (b) The F_{app} values shown are the arithmetic means of the F_{app} values obtained by the three measurements for wild-type (■), P47A (●), P47T (▲), P117G (□), P47A/P117G (○), and P47T/P117G SNase (△). Dotted lines show the theoretical unfolding transition curves.

RESULTS

Stability of Wild-Type and Mutant SNase. The urea-induced unfolding transitions of wild-type SNase and its mutants, P47A, P47T, P117G, P47A/P117G, and P47T/P117G, were measured by difference absorption at 292.5 nm and CD at 225 and 276 nm at pH 7.0 and 20 °C. Figure 1a shows the equilibrium unfolding transition curves for wild-type SNase monitored by these three different measurements. The apparent fraction of native species (F_{app}) is derived from the observed data by the equation

$$F_{app} = \frac{A_{obs} - A_U}{A_N - A_U} \quad (1)$$

where A_{obs} is either the observed ellipticity or the observed difference absorption and A_N and A_U are those values in the

Table 1: Urea-Induced Equilibrium Unfolding Parameters of SNase and Its Mutants at pH 7.0 and 20 °C

protein	C_M (M)	m (kcal mol^{-1} M^{-1})	$\Delta G_U(0)$ (kcal/mol)	$\Delta\Delta G_U = \Delta G_U(2.44)$ (kcal/mol)
wild-type	2.44 ± 0.01	2.09 ± 0.06	5.08 ± 0.14	−
P47A	2.42 ± 0.01	2.05 ± 0.08	4.96 ± 0.19	−0.04 ± 0.02
P47T	2.45 ± 0.01	2.28 ± 0.05	5.60 ± 0.13	0.02 ± 0.02
P117G	3.10 ± 0.02	2.00 ± 0.10	6.19 ± 0.31	1.32 ± 0.11
P47A/P117G	3.02 ± 0.01	2.00 ± 0.06	6.04 ± 0.17	1.16 ± 0.05
P47T/P117G	2.99 ± 0.01	2.12 ± 0.06	6.35 ± 0.17	1.17 ± 0.05

N and U states, respectively. In general, A_N and A_U are dependent on the denaturant concentration, C, and we assume that they are linearly dependent on C; i.e., $A_N = A_{N_1} + A_{N_2}C$, and $A_U = A_{U_1} + A_{U_2}C$. The parameters for the U state, A_{U_1} and A_{U_2}, were calculated from the observed values in the baseline region of the U state. The parameters A_{N_1} and A_{N_2} for the ellipticity at 225 nm were obtained from the data of Kalnin and Kuwajima (1995), and the A_N values for the difference absorption at 292.5 nm and the ellipticity at 276 nm were assumed to be constant ($A_{N_2} = 0$) and calculated from the observed values in the N state. As seen from Figure 1a, the unfolding transition curves measured by the three different spectral probes are coincident with each other within experimental error. Such coincidence of the unfolding transition curves was observed not only in wild-type SNase but also in all the SNase mutants studied. This suggests that the equilibrium unfolding transitions of wild-type and mutant SNase are well represented by a two-state mechanism, in which only the N and U states are populated in the transition zone, as

$$N \overset{K_U}{\rightleftharpoons} U \qquad (2)$$

where K_U is the apparent equilibrium constant for unfolding.

Figure 1b shows the equilibrium unfolding transitions for wild-type SNase and its mutants, P47A, P47T, P117G, P47A/P117G, and P47T/P117G. Each F_{app} value in Figure 1b is the arithmetic mean of the F_{app} values obtained by the three measurements. It can be seen that the unfolding transitions for P47A and P47T are identical to that for wild-type SNase and occur at 2.4 M urea, whereas those for P117G, P47A/P117G, and P47T/P117G are shifted to a higher concentration of urea than the transition for wild-type SNase and have a midpoint of the transition at 3 M urea (Figure 1b), indicating that the P117G mutation has stabilized SNase. To evaluate the stabilities of the proteins more quantitatively, the equilibrium unfolding parameters, the free energy of unfolding (ΔG_U), a cooperativity index of the transition (m), and the denaturant concentration at the midpoint of the unfolding transition (C_M), were calculated from the data of Figure 1b by the method of nonlinear least squares (Pace, 1986; Schellman, 1987; Santoro & Bolen, 1992; Kalnin & Kuwajima, 1995). These parameters are summarized in Table 1. For ΔG_U, the values at 0 and 2.44 M urea are shown in the table. Because 2.44 M urea corresponds to the C_M of wild-type SNase, the ΔG_U at 2.44 M gives a change in the stabilization free energy, $\Delta\Delta G_U$, caused by the mutation for each mutant. Table 1 indicates that the stabilities of the mutants P47A and P47T are identical to that of wild-type SNase, whereas the mutants P117G, P47A/P117G, and P47T/P117G are stabilized by about 1.2 kcal/mol compared with wild-type SNase. Considering the experimental error, the values of m for the five mutants are identical to that for wild-type SNase. The equilibrium unfolding parameters for wild-type SNase are essentially identical to the corresponding values of Kalnin and Kuwajima (1995), which had been obtained by ellipticity at 225 nm under similar conditions. There are several studies on the stability of some of the proline mutants of SNase. Though the experimental conditions used in those studies differ from the present conditions, the relative stabilities of the mutants reported are similar (Green et al., 1992; Nakano et al., 1993). On the other hand, in studies on SNase from the V8 strain, which contains Leu124 instead of His124, the protein was found to be stabilized not only by the substitution of Gly for Pro117 but also by the substitution of Gly for Pro47 (Royer et al., 1993; Truckses et al., 1996; Vidugiris et al., 1996), and this result has been interpreted as evidence of the improvement of the protein packing by the substitutions (Royer et al., 1993).

Kinetics of Refolding and Unfolding. Kinetic refolding and unfolding reactions, which were induced by jumps in urea concentration, were investigated for wild-type and mutant SNase by the stopped-flow absorption and stopped-flow CD techniques. All the kinetic reactions were monitored by the changes of the absorption at 292.5 nm and the ellipticity at 225 nm at pH 7.0 and 20 °C (Figure 2). The refolding and unfolding kinetics of P47T and P47T/P117G were not investigated in the present study, because the kinetics of P47T were found to be identical to those of P47A in a preliminary study (data not shown). Although the data measured by the ellipticity have bigger noise than those by the absorption, the former are less sensitive to systematic errors. The kinetic data were fitted by the nonlinear least-squares method with the equation

$$A(t) = A(\infty) + \Delta A_{obs}\sum_i \alpha_i \exp(-k_i t) \qquad (3)$$

where $A(t)$ and $A(\infty)$ are the observed values of the absorption (or the ellipticity) at time t and infinite time, respectively, ΔA_{obs} is the observed total amplitude [$=A(0) - A(\infty)$], and k_i and α_i are the apparent first-order rate constant and the relative amplitude, respectively, of the ith kinetic phase. These parameters for wild-type SNase and each mutant are plotted as a function of urea concentration (Figure 3). The typical kinetic parameters for wild-type SNase and its mutants are listed in Table 2.

As shown in Figure 3, it was also found that, under every condition studied for wild-type SNase and all its mutants, the rate constants and the relative amplitudes for the refolding and unfolding kinetics of the protein, as measured by the stopped-flow absorption and stopped-flow CD techniques, were identical to each other within experimental error, thus indicating cooperative refolding and unfolding of SNase. In the refolding reaction, however, there must be an additional change occurring in the burst phase, i.e., within the dead time of stopped-flow mixing, because the ΔA_{obs} was smaller than the change expected from the U to the N state, indicating that a burst-phase intermediate was formed at the beginning of refolding. The burst-phase amplitude of the reaction measured by the ellipticity at 225 nm was 30%, which is similar to the amplitude of the reaction measured by the absorption at 292.5 nm (37 ± 10%). For unfolding, there

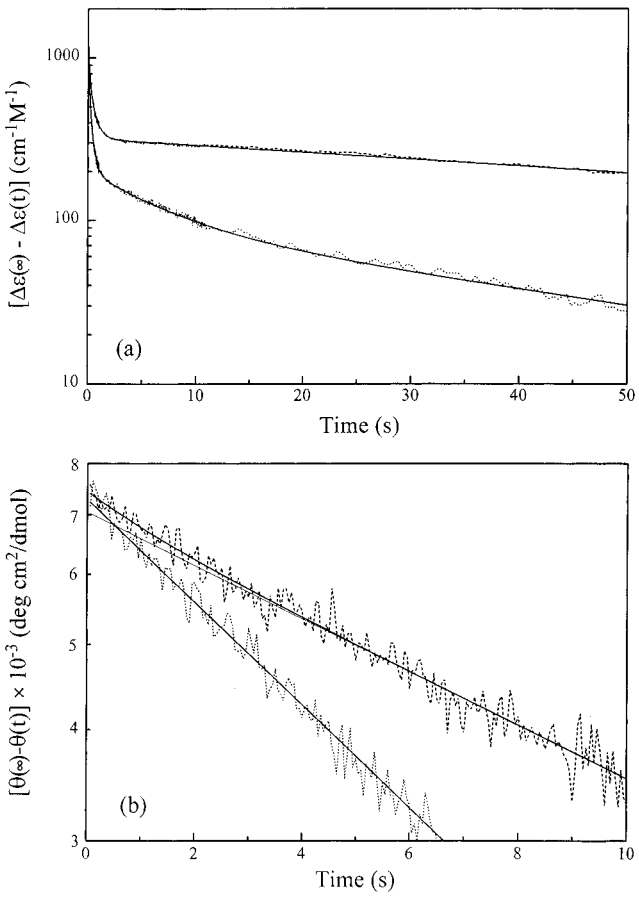

FIGURE 2: Typical kinetic curves of refolding and unfolding for wild-type and P117G SNase at pH 7.0 and 20 °C. The refolding reactions monitored by the absorption at 292.5 nm are shown in panel a, and the unfolding reactions monitored by the CD at 225 nm are shown in panel b. The final urea concentration was 0.45 M for the refolding and 6.1 M for the unfolding. Dashed lines and dotted lines represent the observed kinetic curves for wild-type and P117G SNase, respectively, and thick solid lines represent the theoretical curves fitted to the kinetic data by the nonlinear least-squares method. The slow phase in the unfolding of wild-type SNase is shown by a thin solid line in panel b.

was no burst phase, and the ΔA_{obs} coincided with the change expected from the N to the U state.

Kinetics of Wild-Type SNase. The typical kinetic curves in the refolding and unfolding conditions for wild-type SNase are shown in Figure 2. In refolding, there are at least three phases, the fast, middle, and slow phases. The rate constants of the fast and middle phases are dependent on urea concentration, whereas the rate constant of the slow phase is urea-independent (Figure 3a). The fast and middle phases are major phases in refolding, and the sum of their relative amplitudes is about 80% in the native condition below 1.5 M urea. The relative amplitude of the slow phase is thus about 20% in this condition, but it becomes larger in the transition region.

In the unfolding reaction, two phases were observed (Figure 2b), and the rate constants of both the phases increase with an increase in urea concentration (Figure 3a). The slower of the two phases is the major phase, having a relative amplitude of about 90%.

Several studies have addressed the kinetic refolding and unfolding of wild-type SNase. Although their experimental conditions were not always identical to the present ones, these studies generally observed similar multiphasic refolding kinetics (Chen et al., 1992a,b; Kalnin & Kuwajima, 1995; Nakano et al., 1993; Su et al., 1996; Sugawara et al., 1991). Thus, after employing urea as a denaturant, both Sugawara et al. (1991) and Kalnin and Kuwajima (1995) observed a biphasic unfolding reaction essentially identical to the present one. By contrast, the use of GdnHCl (Su et al., 1996) and GdnSCN (Nakano et al., 1993) as denaturants yielded only a single phase in the unfolding reaction. What caused this discrepancy between the results for different denaturants remains unclear.

Kinetics of P47A. The dependence of the apparent rate constants and the corresponding relative amplitudes on urea concentration for the mutant P47A are shown in Figure 3b. The kinetic profiles for both refolding and unfolding of this mutant were identical to those of wild-type SNase within experimental error. Thus, the mutation of Pro47 does not affect the refolding or unfolding kinetics of SNase.

Kinetics of P117G. The typical kinetic curves for the mutant P117G are also shown and compared with the curves for wild-type SNase in Figure 2. Both the refolding and unfolding reactions for P117G appeared to be faster than those for the wild-type protein. In the refolding kinetics, there are at least four phases, two urea concentration-dependent fast phases and two urea concentration-independent slow phases. The rate constant of the fastest phase and its dependence on urea concentration were very similar to those for wild-type SNase. The rate constant of the second fastest phase was a little larger than that of the middle phase of the wild-type protein. The sum of the relative amplitudes of these phases was about 80% at urea concentrations below 2 M. The rate constants of the slowest and second slowest phases were almost independent of urea concentration, and their relative amplitudes were both about 10%. Although the rate constant of the slowest phase for P117G was almost identical to that of the slow phase for wild-type SNase, its relative amplitude was about half of that of the slow phase for the wild-type protein, suggesting that a portion of the kinetic reactions constituting the slow phase of wild-type SNase has disappeared in P117G. The presence of the two urea concentration-independent slow phases in P117G was not brought about by conformational changes around the other proline residues, caused by the mutation. The X-ray crystallographic structure of the P117G mutant protein has shown that the conformational changes by the mutation are localized around the mutational site (Hynes et al., 1994) and that the position of Pro117 is apart from those of all the other prolines (Hynes & Fox, 1991; Loll & Lattman, 1989).

The unfolding kinetics of P117G were represented by a single-phase reaction, except in the transition region, where biphasic kinetics were seen. This indicates that the above biphasic unfolding for wild-type SNase is caused by the structural heterogeneity attributed to the *cis*/*trans* isomerization about the Lys116−Pro117 peptide bond in the N state and that the *cis* and *trans* forms of the protein may have different unfolding rates.

Other characteristics of P117G, including the coincidence of the observed kinetics measured by the stopped-flow absorption and stopped-flow CD techniques, the presence of the burst phase in refolding, and the absence of the burst phase in unfolding, were the same as in wild-type SNase.

The above results for P117G are consistent with the preliminary results of Kuwajima et al. (1991), although the

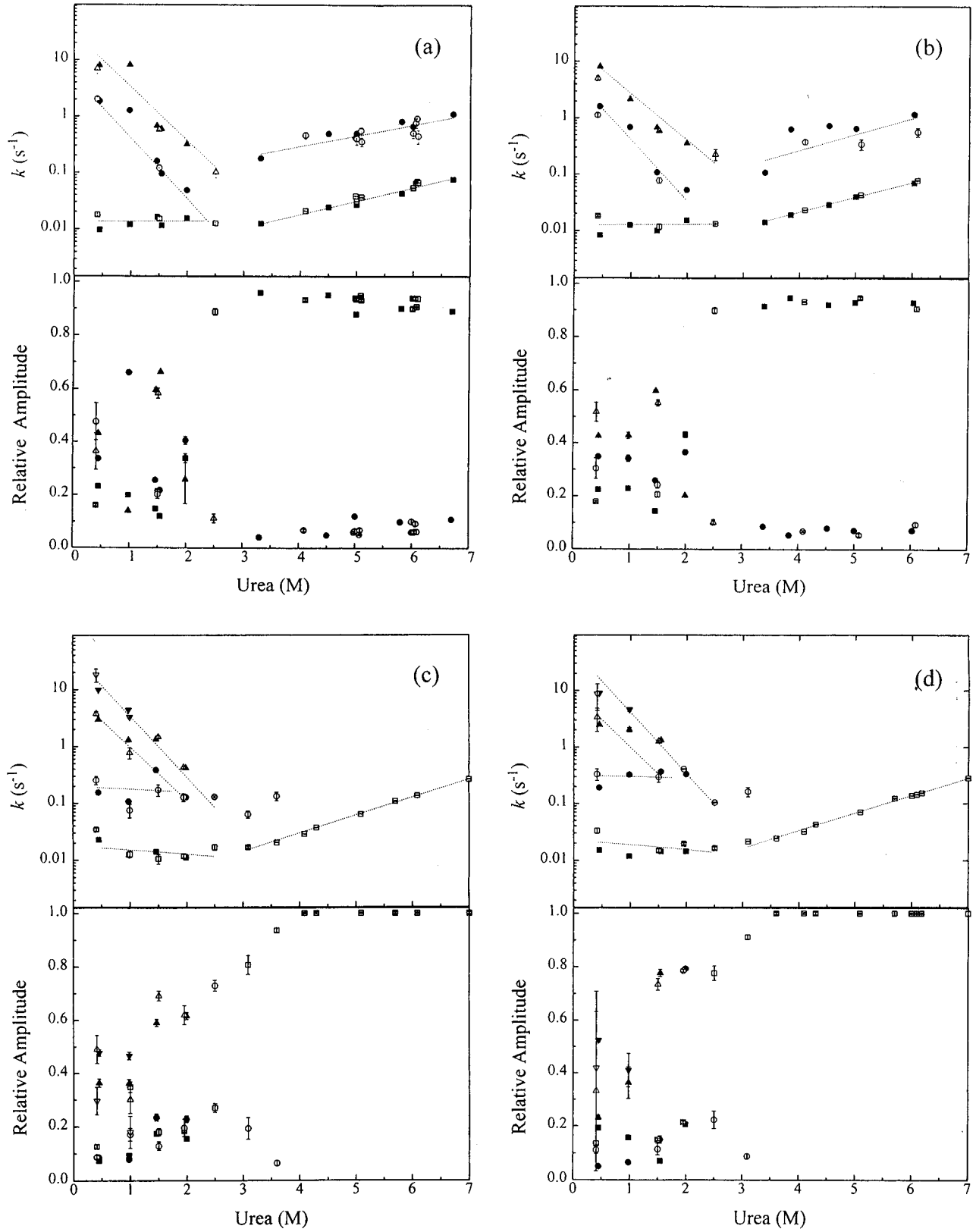

FIGURE 3: Kinetic parameters: the rate constants (upper panel) and the relative amplitudes (lower panel), in the refolding and the unfolding of wild-type (a), P47A (b), P117G (c), and P47A/P117G SNase (d) at pH 7.0 and 20 °C. Open symbols denote the refolding and the unfolding reactions monitored by the CD at 225 nm, and filled symbols denote the refolding and the unfolding reactions monitored by the absorption at 292.5 nm.

temperature is different between the two studies. Nakano et al. (1993) also studied the refolding and unfolding kinetics for P117 mutants at 0 °C and reported complete disappearance of a denaturant (GdnSCN) concentration-independent phase of the refolding by the mutations. It is unknown whether the discrepancy was caused by the difference in denaturants.

Kinetics of P47A/P117G. The dependence of the apparent rate constants and the corresponding relative amplitudes on urea concentration for the mutant P47A/P117G are shown

Table 2: Kinetic Parameters of Refolding and Unfolding for SNase and Its Mutants at pH 7.0 and 20 °C

	rate constant k_i (s^{-1}) and relative amplitude α_i					
	refolding[a]				unfolding[b]	
protein	k_1 (α_1)	k_2 (α_2)	k_3 (α_3)	k_4 (α_4)	k_1 (α_1)	k_2 (α_2)
wild-type	7.95 ± 0.17 (0.432 ± 0.005)	1.86 ± 0.028 (0.336 ± 0.007)	0.0097 ± 0.00010 (0.232 ± 0.002)	−	0.67 ± 0.033 (0.061 ± 0.005)	0.054 ± 0.00018 (0.939 ± 0.005)
P47A	8.09 ± 0.20 (0.426 ± 0.005)	1.62 ± 0.025 (0.349 ± 0.007)	0.0083 ± 0.00013 (0.225 ± 0.003)	−	0.56 ± 0.10 (0.094 ± 0.009)	0.078 ± 0.00090 (0.906 ± 0.008)
P117G	9.84 ± 0.33 (0.477 ± 0.013)	2.98 ± 0.089 (0.363 ± 0.015)	0.15 ± 0.0076 (0.086 ± 0.002)	0.023 ± 0.0010 (0.074 ± 0.002)	0.13 ± 0.00084 (1.000 ± 0.003)	−
P47A/P117G	8.96 ± 0.18 (0.524 ± 0.008)	2.47 ± 0.081 (0.231 ± 0.009)	0.19 ± 0.010 (0.051 ± 0.001)	0.0015 ± 0.00017 (0.193 ± 0.001)	0.14 ± 0.00093 (1.000 ± 0.003)	−

[a] Urea concentration jump of 4.5 → 0.45 M. [b] Urea concentration jump of 1.0 → 6.0 M.

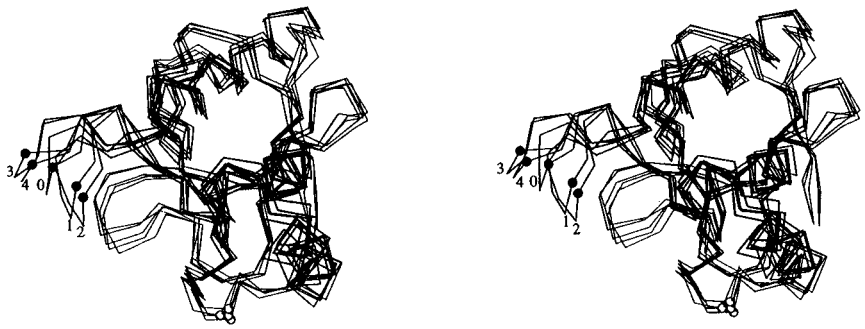

FIGURE 4: Stereoview of four representative snapshots [110 ps (1), 120 ps (2), 140 ps (3), and 200 ps (4)] during the molecular dynamics simulation of wild-type SNase *in vacuo*. The 100−200 ps average structure (0) is also superimposed. The black and white spheres represent the positions of Pro47 and Pro117, respectively.

in Figure 3d. All the characteristics of this mutant were identical to those of P117G within experimental error. Thus, the additional mutation of Pro47 does not affect the refolding and unfolding kinetics of the mutant P117G.

Molecular Dynamics Simulations of Wild-Type SNase. From the present results, the substitution of Ala or Thr for Pro47 does not affect the stability or kinetics, whereas the substitution of Gly for Pro117 increases the stability by about 1.2 kcal/mol and changes the kinetics of unfolding and refolding. In order to investigate whether the difference of the mutational effects for Pro47 and Pro117 is related to the difference of the structural dynamics around these residues, we carried out molecular dynamics simulations for wild-type SNase. The crystal structure of wild-type SNase without metal ion and inhibitor (1STN; Hynes & Fox, 1991) was chosen as an initial structure. Because the crystal coordinates of the N-terminal residues from 1 to 5 and the C-terminal residues from 142 to 149 were not reported, the structure used in the simulation does not contain these residues. The molecular dynamics simulations were first carried out *in vacuo*, where the inherent characteristics of protein dynamics are most easily observed. After the system was equilibrated for 100 ps at 20 °C (293 K), transient structures were collected every 1 ps. Figure 4 shows the C^α traces of five representative structures observed in the simulations. Although the global conformation was stable over the simulation time (200 ps), there were six regions which showed large displacements (more than 1 Å) from the average position: residues 6−11, 28−30, 43−52, 70−72, 78−86, and 127−141 (see the Supporting Information). With the exception of residues 6−11 (N-terminal) and 127−141 (C-terminal), all the regions were located in loops or turns. The displacements of C^α atoms for residues 43−52 were largest (the maximum value is 6.5 Å at Lys48), which suggests that this region is most flexible. By contrast, the displacements for the residues around Pro117 were small (1 Å at most) (Figure 4).

The molecular dynamics simulations of the protein were also carried out in a rectangular box that contained 4041 water molecules, under a periodic boundary condition. The temperature of the system was increased to 327 K, which was the experimental denaturation temperature at neutral pH. As in the simulations *in vacuo*, a 100 ps trajectory was studied after 100 ps of equilibration. The displacements of C^α atoms for residues 43−52 were larger than those for the rest of the protein, although they were $^1/_3$ of the magnitude of those observed *in vacuo* (see the Supporting Information).

In summary, the molecular dynamics simulations both *in vacuo* and in water show the extraordinarily high flexibility of the residues around Pro47. This flexibility is about 6 times (*in vacuo*) or 2 times (in water) higher than the flexibility of the region around Pro117 in the 100 ps trajectories of the simulations.

DISCUSSION

It has been well documented that *cis*/*trans* isomerizations about X−Pro peptide bonds occur in the U state of a protein and relate to slow steps in protein folding (Brandts et al., 1975; Kiefhaber et al., 1992; Kiefhaber & Schmid, 1992; Kim & Baldwin, 1982). Recent studies have, however, also demonstrated that some proteins show isomerization about an X−Pro peptide bond in the N state, which gives rise to structural heterogeneity in the N state (Amodeo et al., 1994; Chazin et al., 1989; Shalongo et al., 1993). The His46−Pro47 and Lys116−Pro117 bonds of SNase afford the best-characterized examples of such prolyl peptide bonds, and the isomerizations about these bonds have been studied by NMR spectroscopy, site-directed mutagenesis, size-exclusion

chromatography, and computational analysis (Alexandrescu et al., 1988, 1989, 1990; Eftink et al., 1989; Evans et al., 1987, 1989; Fox et al., 1986; Hinck et al., 1993; Hodel et al., 1993, 1995a,b; Kuwajima et al., 1991; Loh et al., 1991; Nakano et al., 1993; Raleigh et al., 1992; Royer et al., 1993; Shalongo et al., 1992; Vidugiris et al., 1996; Truckses et al., 1996; Wang et al., 1990). The isomerizations about these two peptide bonds of SNase occur independently and produce the four different native conformers. Such structural heterogeneity of native SNase may significantly affect the unfolding and refolding reactions of the protein. Thus, we have constructed five prolyl mutants (P47A, P47T, P117G, P47A/P117G, and P47T/P117G) and studied the equilibrium and kinetics of refolding and unfolding of the proteins. As expected, the effect of the mutation at Pro117 is independent of those of the mutations at Pro47. Rather surprisingly, however, the mutational effects on the refolding and unfolding of SNase are remarkably different between the two sites. The P47A and P47T mutations neither change the stability of SNase nor affect the kinetics of the refolding and unfolding, while the P117G mutation increases the protein stability and affects both the refolding and unfolding kinetics. This difference may not arise from the difference of the amino acid residues after the mutations but rather from the difference of the structures around the two mutation sites, because the P117T mutation is also known to increase the protein stability (Nakano et al., 1993). In order to investigate the difference of the structures around Pro47 and Pro117, we carried out molecular dynamics simulations of SNase and found a remarkable difference in flexibility between the structures around Pro47 and Pro117. In the following, we first discuss the structural dynamics and proline isomerization of native SNase and then discuss the folding scheme of the protein deduced from the experimental data of the kinetic unfolding and refolding of wild-type and mutant SNase.

Structural Dynamics and Proline Isomerization of SNase. The molecular dynamics simulations of wild-type SNase have revealed similar dynamic features of the native SNase structure *in vacuo* and in water, although the motions of the protein in water are dumped considerably by surrounding water molecules. In general, loops and turns are more flexible than the rest of the protein. In particular, the loop around Pro47 shows the highest flexibility and is much more flexible than the turn around Pro117 (Figure 4).

It is thus very likely that the extraordinarily high flexibility of the loop around Pro47, as also suggested in the previous X-ray crystallographic (Hynes & Fox, 1991; Loll & Lattman, 1989) and NMR (Alexandrescu et al., 1996; Kay et al., 1989) studies, is the reason why the mutations at Pro47 neither change the stability of SNase nor affect the kinetics of the unfolding and refolding. Probably the local structure of the loop around Pro47 is "unfolded-like" even in the N state. This inference is supported by the fact that the fraction of the *cis* isomer of the Pro47 peptide bond in the N state is about 20% as estimated by the NMR study (Loh et al., 1991), because this value is the same as the fraction of the *cis* isomer of an X−Pro peptide bond generally expected in the U state (Brandts et al., 1975; Creighton, 1980; Raleigh et al., 1992). The single-phase unfolding kinetics of P117G also indicate that the isomerization of the Pro47 peptide bond is not related to the unfolding of SNase, supporting the view that the local structure around Pro47 is already unfolded-like in the N state, so that the isomerization occurs without restraint and does not affect the unfolding kinetics.

In contrast to the nonrestraint isomerization of the Pro47 peptide bond mentioned above, the isomerization of the Pro117 peptide bond is accompanied by a nonlocal conformational change in the N state (Evans et al., 1989), because the region around Pro117 is not flexible (see Figure 4). The conformational difference of the isomers of Pro117 may bring about a difference in the unfolding kinetics between the isomers. In fact, biphasic unfolding kinetics were observed in wild-type SNase and the mutants containing Pro117, and each of the two phases of the biphasic unfolding may correspond to the unfolding of each of the two native isomers (Kuwajima et al., 1991). The *cis* to *trans* isomerization rate of X−Pro peptide bonds in linear and cyclic peptides has been estimated to be on the order of 10^{-3} s^{-1} at 25 °C (Grathwoel & Wüthrich, 1981), which is slower than the unfolding rate of SNase, and the isomerization of the Lys116−Pro117 peptide bond must be further slowed by the rigid structure around this bond. Therefore, the unfolding reactions of the two isomers occur independently, and without interconversion. Comparing the relative amplitudes of the two phases with populations of the *cis* and *trans* native isomers shown in the NMR studies (Evans et al., 1989; Alexandrescu et al., 1989), we note that the reaction represented by the fast phase corresponds to the unfolding of the *trans* isomer and the reaction represented by the slow phase corresponds to that of the *cis* isomer.

Folding Scheme of SNase. The kinetic refolding studies of wild-type and all the mutant SNase have revealed rapid accumulation of a partially folded species as soon as the refolding starts from the U state, and the simplest scheme that represents the refolding of SNase from the partially folded state is

Scheme 1

$$\mathrm{D} \longrightarrow \mathrm{N}$$

where D denotes the partially folded state (the denatured state in the native condition) to which the protein refolds within the dead time of the stopped-flow measurements (less than 20 ms) (Sugawara et al., 1991; Kalnin & Kuwajima, 1995). Here, we use the notation D to distinguish this state from the fully unfolded state in concentrated urea. In the stopped-flow CD measurement at 225 nm, the fractional ellipticity change from U to D relative to the ellipticity change for the overall refolding from the U to N state is 30% (Sugawara et al., 1991), and this value is remarkably smaller than the corresponding values (more than 80%) for α-lactalbumin, lysozyme, and other proteins (Goldberg, 1990; Kuwajima et al., 1985, 1987, 1988).

The real refolding reaction of SNase must be, however, more complicated than the pathway shown in Scheme 1, because the multiphasic kinetics were observed in the refolding of the protein. In general, such multiphasic kinetics are represented by a sequential pathway (e.g., $\mathrm{D} \rightarrow \mathrm{I}_1 \rightarrow \mathrm{I}_2 \rightarrow \cdots \rightarrow \mathrm{N}$) or multiple parallel pathways (e.g., $\mathrm{D}_1 \rightarrow \mathrm{N}$, $\mathrm{D}_2 \rightarrow \mathrm{N}$, ⋯). The refolding of SNase is well represented by the parallel pathways, because the kinetics measured by different structural probes, the peptide ellipticity at 225 nm and the tryptophan absorption at 292.5 nm, are coincident with each other, indicating that the refolding from D to N is a cooperative process without intermediate states. In fact,

considering the heterogeneity produced by isomerizations about the Pro47 and Pro117 peptide bonds in the N state, four different native conformers must be present after the refolding. However, the *cis*/*trans* isomerization about the Pro47 peptide bond does not affect the refolding kinetics (see above), and the isomerization about this bond should be ignored. Thus, when we consider only the isomerization about the Pro117 peptide bond for wild-type SNase, the refolding reaction of the protein can be tentatively represented by

Scheme 2

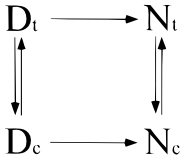

where the subscripts c and t represent the *cis* and *trans* isomers of the Pro117 peptide bond, respectively. Each of the fast and middle phases in the refolding of wild-type SNase can be assigned to either of the $D_t \rightarrow N_t$ and $D_c \rightarrow N_c$ processes. The slow phase can be attributed to the isomerization process $D_t \rightleftarrows D_c$. The isomerization process $N_t \rightleftarrows N_c$ is "silent" in the refolding of wild-type SNase; there is no difference in either the ellipticity or the absorption between the N_t and N_c states. In this manner, Scheme 2 gives an explanation of the observed refolding kinetics of wild-type SNase.

If the folding reaction of SNase is represented by Scheme 2, the refolding of the mutants in which Pro117 is replaced by Gly must be a single-phase reaction. In the real refolding of the mutant proteins (P117G and P47A/P117G), however, there are apparently four kinetic phases observed, two urea concentration-dependent fast phases and two urea concentration-independent slow phases. The urea concentration-independent slower phases may arise from isomerization reactions of at least two other proline residues or other isomerization events such as domain rearrangement with little or no net change in the exposure of side chains and backbone to solvent in the D state (Mann et al., 1995). Assuming the slow phases arise from the *cis*/*trans* isomerizations of two other proline residues, the folding of P117G and P47A/P117G may be represented by

Scheme 3

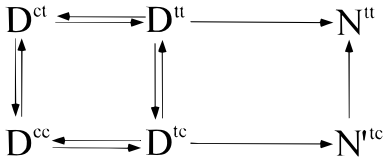

where the superscripts c and t represent the *cis* and *trans* isomers about two prolines other than Pro47 and Pro117 and the N'^{tc} state is a transient native-like state that involves a non-native *cis* proline. The structure is almost native in the N'^{tc} state, and there is no difference in the ellipticity or absorption between N^{tt} and N'^{tc}. In order to simplify the scheme, we do not take into account of the existence of other native-like states that involve one or two non-native *cis* proline(s), such as N'^{cc} and N'^{ct}. Thus, in this scheme, the molecule in the D^{ct} or D^{cc} states cannot directly refold to the N state but must refold via the isomerization processes in the D state. Therefore, each of the two urea concentration-dependent phases corresponds to either of the $D^{tt} \rightarrow N^{tt}$ and $D^{tc} \rightarrow N'^{tc}$ processes, and the two urea concentration-independent phases are ascribed to the proline isomerization processes in the D state. To ascertain the role of proline isomerization in the urea concentration-independent slow phases, we estimated activation enthalpies of these phases from the present data at 20 °C and the previous data for refolding of P117G at 4.5 °C (Kuwajima et al., 1991). The activation enthalpies obtained were from 11.8 to 32.8 kcal/mol (20 °C), which were in agreement with that expected for proline isomerization (Brandts et al., 1975).

As a result, the folding reaction of wild-type SNase is represented by the following scheme, which is a combination of Schemes 2 and 3:

Scheme 4

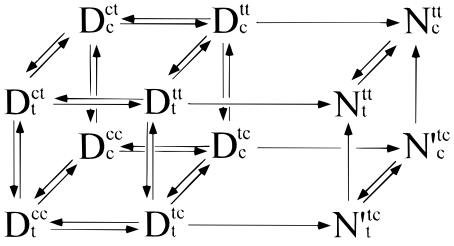

where both the $N_t'^{tc}$ and $N_c'^{tc}$ states are transient native-like states that involve a non-native *cis* proline. Although there are four processes, $D_t^{tt} \rightarrow N_t^{tt}$, $D_c^{tt} \rightarrow N_c^{tt}$, $D_t^{tc} \rightarrow N_t'^{tc}$, and $D_c^{tc} \rightarrow N_c'^{tc}$, that may depend on urea concentration, only two kinetic phases were observed experimentally (Figure 3). In Scheme 4, although there are 12 proline isomerizations, only one urea concentration-independent phase was observed experimentally. The cause of this degeneracy in observation remains obscure, but it may involve the similarity of the rate constants of different kinetic processes.

In Schemes 3 and 4, we assumed that the isomerizations observed in the refolding of the P117G and P47A/P117G mutants were attributed to *cis*/*trans* isomerizations of other proline residues. In order to confirm the validity of this assumption, however, it will be necessary to examine the folding kinetics of the mutants by a series of complex double-mixing experiments, the folding kinetics of other proline mutants of SNase, and the effect of peptidyl-prolyl *cis*/*trans* isomerase on the slow phases.

ACKNOWLEDGMENT

The authors are grateful to Prof. I. Kumagai (University of Tokyo) for his valuable suggestions and his donation of plasmid pUT7 and to Mr. S. Mizutani (University of Tokyo) for his assistance with the construction of the expression vector pMT7.

SUPPORTING INFORMATION AVAILABLE

Three figures showing structural dynamics of wild-type SNase, with two of those figures derived from the molecular dynamics simulations *in vacuo* and in water compared with the figure derived from the X-ray crystallographic studies (4 pages). Ordering information is given on any current masthead page.

REFERENCES

Alexandrescu, A. T., Mills, D. A., Ulrich, E. L., Chinami, M., & Markley, J. L. (1988) *Biochemistry 27*, 2158−2165.

Alexandrescu, A. T., Ulrich, E. L., & Markley, J. L. (1989) *Biochemistry 28*, 204−211.

Alexandrescu, A. T., Hinck, A. P., & Markley, J. L. (1990) *Biochemistry 29*, 4516−4525.

Alexandrescu, A. T., Jahnke, W., Wiltscheck, R., & Blommers, M. J. J. (1996) *J. Mol. Biol. 260*, 570−587.

Amodeo, P., Morelli, M. A. C., & Motta, A. (1994) *Biochemistry 33*, 10754−10762.

Anfinsen, C. B. (1973) *Science 181*, 223−230.

Arai, M., & Kuwajima, K. (1996) *Folding Des. 1*, 275−287.

Baldwin, R. L. (1993) *Curr. Opin. Struct. Biol. 3*, 84−91.

Baldwin, R. L. (1996) *Folding Des. 1*, R1−R8.

Brandts, J. F., Halvorson, H. R., & Brennan, M. (1975) *Biochemistry 14*, 4953−4963.

Bryngelson, J. D., Onuchic, J. N., Socci, N. D., & Wolynes, P. G. (1995) *Proteins 21*, 167−195.

Chazin, W. J., Kördel, J., Drakenberg, T., Thulin, E., Brodin, P., Grundström, T., & Forsén, S. (1989) *Proc. Natl. Acad. Sci. U.S.A. 86*, 2195−2198.

Chen, B.-L., Baase, W. A., & Schellman, J. A. (1989) *Biochemistry 28*, 691−699.

Chen, H. M., Markin, V. S., & Tsong, T. Y. (1992a) *Biochemistry 31*, 1483−1491.

Chen, H. M., Markin, V. S., & Tsong, T. Y. (1992b) *Biochemistry 31*, 12369−12375.

Creighton, T. E. (1980) *J. Mol. Biol. 137*, 61−80.

Dill, K. A., Bromberg, S., Yue, K., Fiebig, K. M., Yee, D. P., Thomas, P. D., & Chan, H. S. (1995) *Protein Sci. 4*, 561−602.

Eftink, M. R., Ghiron, C. A., Kautz, R. A., & Fox, R. O. (1989) *Biophys. J. 55*, 575−579.

Evans, P. A., Dobson, C. M., Kautz, R. A., Hatfull, G., & Fox, R. O. (1987) *Nature 329*, 266−268.

Evans, P. A., Kautz, R. A., Fox, R. O., & Dobson, C. M. (1989) *Biochemistry 28*, 362−370.

Fox, R. O., Evans, P. A., & Dobson, C. M. (1986) *Nature 320*, 192−194.

Goldberg, M. E., Semisotnov, G. V., Friguet, B., Kuwajima, K., Ptitsyn, O. B., & Sugai, S. (1990) *FEBS Lett. 263*, 51−56.

Grathwohl, C., & Wüthrich, K. (1981) *Biopolymers 20*, 2623−2633.

Green, S. M., Meeker, A. K., & Shortle, D. (1992) *Biochemistry 31*, 5717−5728.

Hinck, A. P., Eberhardt, E. S., & Markley, J. L. (1993) *Biochemistry 32*, 11810−11818.

Hodel, A., Kautz, R. A., Jacobs, M. D., & Fox, R. O. (1993) *Protein Sci. 2*, 838−850.

Hodel, A., Kautz, R. A., & Fox, R. O. (1995a) *Protein Sci. 4*, 484−495.

Hodel, A., Rice, L. M., Simonson, T., Fox, R. O., & Bruenger, A. T. (1995b) *Protein Sci. 4*, 636−654.

Hynes, T. R., & Fox, R. O. (1991) *Proteins 10*, 92−105.

Hynes, T. R., Hodel, A., & Fox, R. O. (1994) *Biochemistry 33*, 5021−5030.

Jorgensen, W. L., Chandrasekhar, H., Madura, J. D., Impey, R. W., & Klein, M. L. (1983) *J. Chem. Phys. 79*, 926−935.

Kalnin, N. N., & Kuwajima, K. (1995) *Proteins 23*, 163−176.

Kay, L. E., Torchia, D. A., & Bax, A. (1989) *Biochemistry 28*, 8972−8979.

Kiefhaber, T., & Schmid, F. X. (1992) *J. Mol. Biol. 224*, 231−240.

Kiefhaber, T., Kohler, H.-H., & Schmid, F. X. (1992) *J. Mol. Biol. 224*, 217−229.

Kim, P. S., & Baldwin, R. L. (1982) *Annu. Rev. Biochem. 51*, 459−489.

Kim, P. S., & Baldwin, R. L. (1990) *Annu. Rev. Biochem. 59*, 631−660.

Kunkel, T. A. (1985) *Proc. Natl. Acad. Sci. U.S.A. 82*, 488−492.

Kuwajima, K. (1989) *Proteins 6*, 87−103.

Kuwajima, K. (1996) *FASEB J. 10*, 102−109.

Kuwajima, K., Hiraoka, Y., Ikeguchi, M., & Sugai, S. (1985) *Biochemistry 24*, 874−881.

Kuwajima, K., Yamaya, H., Miwa, S., Sugai, S., & Nagamura, T. (1987) *FEBS Lett. 221*, 115−118.

Kuwajima, K., Sakuraoka, A., Fueki, S., Yoneyama, M., & Sugai, S. (1988) *Biochemistry 27*, 7419−7428.

Kuwajima, K., Okayama, N., Yamamoto, K., Ishihara, T., & Sugai, S. (1991) *FEBS Lett. 290*, 135−138.

Kuwajima, K., Yamaya, H., & Sugai, S. (1996) *J. Mol. Biol. 264*, 806−822.

Lee, B., & Richards, F. M. (1971) *J. Mol. Biol. 55*, 379−400.

Levinthal, C. (1968) *J. Chem. Phys. 65*, 44−45.

Loh, S. N., McNemar, C. W., & Markley, J. L. (1991) *Techniques in Protein Chemistry*, Vol. 2, pp 275−282, Academic Press, San Diego.

Loll, P. J., & Lattman, E. E. (1989) *Proteins 5*, 183−201.

Mann, C. J., Shao, X., & Matthews, C. R. (1995) *Biochemistry 34*, 14573−14580.

Miranker, A. D., & Dobson, C. M. (1996) *Curr. Opin. Struct. Biol. 6*, 31−42.

Nakano, T., Antonino, L. C., Fox, R. O., & Fink, A. L. (1993) *Biochemistry 32*, 2534−2541.

Onuchic, J. N., Wolynes, P. G., Luthy-Schulten, Z., & Socci, N. D. (1995) *Proc. Natl. Acad. Sci. U.S.A. 92*, 3626−3630.

Pace, C. N. (1986) *Methods Enzymol. 131*, 266−280.

Raleigh, D. P., Evans, P. A., Pitkeathly, M., & Dobson, C. M. (1992) *J. Mol. Biol. 228*, 338−342.

Richmond, T. J. (1984) *J. Mol. Biol. 178*, 63−89.

Royer, C. A., Hinck, A. P., Loh, S. N., Prehoda, K. E., Peng, X., Jonas, J., & Markley, J. L. (1993) *Biochemistry 32*, 5222−5232.

Saiki, R. K., Gelfand, D. H., Stoffel, S., Scharf, S. J., Higuchi, R., Horn, G. T., Mullis, K. B., & Erlich, H. A. (1988) *Science 239*, 487−491.

Santoro, M. M., & Bolen, D. W. (1992) *Biochemistry 31*, 4901−4907.

Sayers, J. R., Schmidt, W., & Eckstein, F. (1988) *Nucleic Acids Res. 16*, 791−802.

Schellman, J. A. (1987) *Annu. Rev. Biophys. Biophys. Chem. 16*, 115−137.

Scheraga, H. A. (1996) *Biophys. Chem. 59*, 329−339.

Shalongo, W., Jagannadham, M. V., Heid, P., & Stellwagen, E. (1992) *Biochemistry 31*, 11390−11396.

Shalongo, W., Jagannadham, M., & Stellwagen, E. (1993) *Biopolymers 33*, 903−913.

Su, Z. D., Arooz, M. T., Chen, H. M., Gross, C. J., & Tsong, T. Y. (1996) *Proc. Natl. Acad. Sci. U.S.A. 93*, 2539−2544.

Sugawara, T., Kuwajima, K., & Sugai, S. (1991) *Biochemistry 30*, 2698−2706.

Tanaka, A., Flanagan, J., & Sturtevant, J. M. (1993) *Protein Sci. 2*, 567−576.

Truckses, D. M., Somoza, J. R., Prehoda, K. E., Miller, S. C., & Markley, J. L. (1996) *Protein Sci. 5*, 1907−1916.

Tucker, P. W., Hazen, E. E., Jr., & Cotton, F. A. (1978) *Mol. Cell. Biochem. 22*, 67−77.

Verlet, L. (1967) *Phys. Rev. 159*, 98−103.

Vidugiris, G. J. A., Truckses, D. M., Markley, J. L., & Royer, C. A. (1996) *Biochemistry 35*, 3857−3864.

Wang, J., Hinck, A. P., Loh, S. N., & Markley, J. L. (1990) *Biochemistry 29*, 4242−4253.

BI963174V